Chains of temporal dark solitons in dispersion-managed fiber

M. Stratmann and F. Mitschke*
Institut für Physik, Universität Rostock, Rostock, Germany
(Received 28 September 2005; published 28 December 2005)

Attractive interaction of dark dispersion-managed (DM) solitons is observed numerically. For certain initial separations chains of bound dark DM solitons are found. The chains can have various lengths (up to 12 solitons are shown), and the nearest-neighbor separations can take several values—all the same or mixed.

DOI: 10.1103/PhysRevE.72.066616 PACS number(s): 42.81.Dp, 42.65.Tg, 42.79.Sz

I. SOLITONS IN FIBER

Bright solitons in optical fiber are pulses of light with a hyperbolic-secant envelope shape (sech^2 power profile) and a specific relation between peak power and duration. Since the suggestion [1] and experimental demonstration [2], uncounted studies have given us a fairly complete understanding; today solitons are entering deployment in commercial telecommunications systems. The mathematical background is that bright solitons are stable solutions of the underlying wave equation, the nonlinear Schrödinger equation (NLSE) [3,4]

$$\frac{\partial A}{\partial z} = -\frac{i}{2}\beta_2 \frac{\partial^2 A}{\partial T^2} + i\gamma |A|^2 A \tag{1}$$

where $A(z,T)$ is the pulse envelope, z is the coordinate in the propagation direction, T is time in the comoving frame, and β_2 and γ are the coefficients for dispersion and nonlinearity, respectively. Stability of the solution implies self-correcting effects after perturbation; hence the appeal of solitons as the natural "bits" for optical telecommunication.

To better approximate realistic conditions, additional terms are often added to the NLSE to account for higher order dispersion, Raman effect, two-photon absorption, or other effects. It has been shown that solitons remain stable in the presence of Hamiltonian deformations, but decay over finite distances when there are non-Hamiltonian perturbations [5]. In the real world, of course, all distances are finite, and telecom fibers are unlikely to be longer than the half perimeter of this planet. We will call mathematically unstable solutions *quasistable* when the decay can be scaled beyond any practically relevant distance. Quasistable solutions are still viable for applications, even though the self-healing properties are compromised. We note in passing that numerical studies can, at best, prove quasistability.

Even in its most basic form the NLSE allows a variety of solutions other than the bright soliton. Not counting the trivial and the cw solutions [4], arguably the most relevant is the dark soliton. Actually there is a whole family of dark solitons with varying grades of darkness (gray solitons), but it has become customary to designate as "dark soliton" what more precisely would be called the "black soliton" [4]. We will not discuss shades of gray other than black. Dark solitons are stable solutions in the regime of normal dispersion. They have a hyperbolic-tangent envelope shape ($\tanh^2$ or inverted sech^2 power profile) and sit on an infinitely wide bright background. While the first experimental demonstrations [6,7] followed soon after that of the bright soliton, the number of experimental studies devoted to the dark soliton case [6–9] is quite limited. One reason is that dark solitons are more difficult to generate.

Some authors have argued that dark solitons are more stable in the presence of perturbations due to their phase jump which, being a topological singularity, cannot be lifted by smooth deformation. Also, they are less susceptible to perturbations from loss [10,11], the Gordon-Haus effect [12,13], or interactions [14] than their bright counterparts. On the other hand it has been shown that the Raman effect, which for bright solitons nondestructively shifts the frequency [15], shifts dark solitons in more complicated ways and ultimately destroys them [16,17]. In any event, the broad (in principle, infinitely broad) background required for dark solitons creates both an increased demand for power and an enhanced risk of Brillouin scattering. Therefore, practical systems so far have used bright solitons exclusively. Nonetheless, dark solitons remain an amazing subject from a fundamental point of view. It is also possible that in dispersion-managed fiber (see below) their inherent drawbacks need to be revisited: conclusions based on the conventional fiber case might be premature.

For our present purposes we also need to mention solutions of the NLSE that take the form of Jacobi elliptical functions. They are summarily called "cnoidal waves" and describe infinite trains of bright (*cn*, *dn*) or dark (*sn*) pulses. The *sn* solution is stable in normal dispersion, and can be stable or quasistable in the presence of the Raman effect [18]. Very recently even solutions of a dark soliton on top of a cnoidal wave were found [19].

In this paper we describe coupled states of dark solitons. We do not consider coupling between solitons of different optical frequencies or of different polarization states, but deal with same-frequency, same-polarization solitons exclusively.

II. DISPERSION MANAGEMENT

As it turns out, today very often fibers are deployed which do not have a constant dispersion value along its entire stretch (called homogeneous fiber henceforth), but rather al-

*Electronic address: fedor.mitschke@uni-rostock.de

ternates between positive and negative dispersion [in Eq. (1), $\beta_2 \rightarrow \beta_2(z)$]. Such dispersion-managed (DM) fibers have several advantages for optical data transmission, not the least among which is the nearly complete suppression of four wave mixing which otherwise would generate severe channel cross talk in wavelength-division multiplexed systems.

It has been established in Refs. [20–24] that bright solitons exist in such fibers, but with slightly modified shape and interaction behavior in comparison to their counterparts in homogeneous fibers. They are thus referred to as DM solitons. A corresponding result was obtained for dark solitons [25] and confirmed semianalytically in [26], and it was specifically pointed out that dark DM solitons have characteristic undulations in their wings that are much more pronounced than for bright DM solitons. These undulations are important for our present purpose.

Dispersion management is typically done by assigning alternating dispersion values in a strictly periodical fashion. It has been established, however, that small deviations from such exact periodicity, while unavoidable when several segments of fiber are concatenated in practice, do not upset the bright DM soliton format [27] in the sense that they remain quasistable.

Several facts are quite different in DM fibers, as compared to homogenous fibers: In DM fiber, all solitons are periodically perturbed, and this fact changes their stability properties considerably. Both bright and dark DM solitons are only quasistable. Cnoidal waves of the *cn* and *dn* type in homogenous fibers are unstable over wide ranges of parameter space [29]. However, in DM their stability properties are different: *cn* waves experience reduced instability and may be called quasistable, while the stability of *sn* waves is degraded from stable to quasistable [30]. Moreover, entirely new classes of solitonlike solutions exist in DM fibers. Recently soliton molecules, consisting of bound states of bright and dark solitons, were discovered numerically, then demonstrated experimentally [28]. Such a compound state would be highly unstable in homogenous fibers.

III. BOUND DARK SOLITONS

In this paper we introduce a family of quasistable solutions. We present a numerical study of the interaction between temporal dark DM solitons. We report that dark solitons in DM fiber lines exhibit not only repulsive but also attractive interaction—this is quite different from the situation in homogeneous fiber. Then we show the existence of stable bound states of dark DM solitons. Finally, we demonstrate that these bound states can take the form of chains of several dark solitons.

It has been known [31] that dark (black) fiber solitons always repel; [32] extend this to both black and gray solitons. For bright DM solitons bound states have been discussed before. Paré and Bélanger theoretically pointed out the possibility of soliton pairs [33], and Maruta found compounds of more than two solitons [34]. An experimental observation of a DM soliton compound was reported in Ref. [28]. We will comment on the relation of our finding to a theoretical study of dispersion-managed cnoidal waves [30] below.

IV. PROCEDURE

To compute the propagation of dark DM solitons we numerically solve the NLSE by applying the well-known split-step Fourier method [4]. We let the dispersion coefficient β_2 alternate between $\beta_2=\beta_+$ and $\beta_2=\beta_-$ for lengths L_+ and L_-, respectively. The important characteristics of a dispersion-managed fiber are the dispersion map period $L_{\mathrm{map}}=L_++L_-$, the path average dispersion

$$\bar{\beta}_2 = \frac{\beta_+ L_+ + \beta_- L_-}{L_{\mathrm{map}}},$$

and the map strength

$$S = \frac{|\beta_+ - \bar{\beta}_2| L_+ + |\beta_- - \bar{\beta}_2| L_-}{\tau^2}.$$

Here τ is the full width at half minimum (FWHM). For consistency, we will henceforth refer all dark pulse widths to the FWHM of a single dark soliton after initial transients have died down, which we call τ_{sol}. We keep the nonlinearity parameter γ constant, and we do not include higher order effects, gain, or polarization effects.

In simulations of dark solitons one needs to replace the infinite cw background with a finite background pulse. This background pulse has to be much wider than the dark pulse, indeed so broad that no artifacts from its wings become noticeable. We use here an unchirped super-Gaussian (with exponent 6) background pulse 200 times wider than the dark soliton in order to assure an almost constant background level, in a computational window another factor of four wider than that. We convinced ourselves by varying the width of the background that for these parameters, artifacts caused by the finite width of the background pulse are avoided.

We simulated transmission lines consisting of $100\cdots300$ map periods. For dark pulse widths of about 1 ps width, this corresponds to a total span length of $20\cdots60$ km. The length is better expressed in units of characteristic dispersion lengths L_{D}; we use the definition $L_{\mathrm{D}}=(0.567\tau_{\mathrm{sol}})^2/|\bar{\beta}_2|$. Then our simulations span $31\cdots93$ L_{D}. The length can also be expressed in units of nonlinear lengths, defined as $L_{\mathrm{NL}}=1/(\gamma P_0)$ with P_0 the power of the background; then our simulations cover the range of $77\cdots231$ L_{NL}.

In real-world units, to generate a single dark soliton we launch a tanh-shaped envelope pulse with an initial FWHM of the dip in the power profile of $\tau=1$ ps and let it propagate in a path-average dispersion of $\bar{\beta}_2=1$ ps^2/km. The map strength of the fiber line was $S=1.8$. Over the first ≈10 dispersion lengths or so this initial pulse develops into a dark DM soliton with a FWHM of $\tau_{\mathrm{sol}}=1.43$ ps.

V. DARK SOLITON PAIRS

We turn to the mutual interaction in a pair of dark solitons. To this end we use the product of two position-shifted dark pulses as described above as a launch condition. It should be clear that this shape is only a rough approximation to the dark soliton pair shape. In Fig. 1 the separation of the

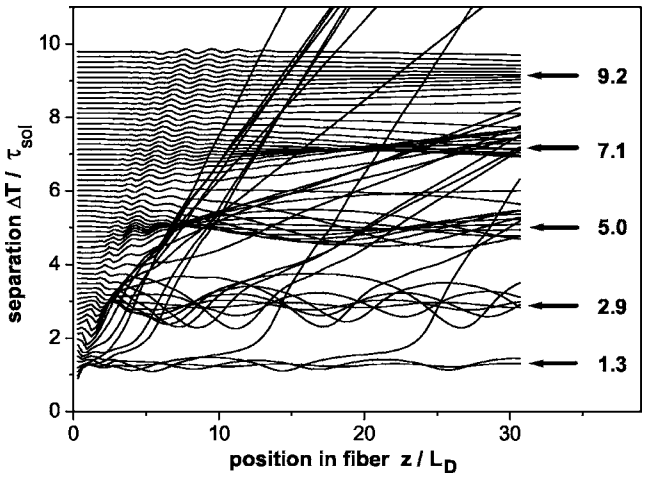

FIG. 1. Interaction of two dark DM solitons: separation $\Delta T/\tau_{\mathrm{sol}}$ as a function of propagation distance z/L_{D}. The separations evolve towards a discrete set of equilibrium values (arrows).

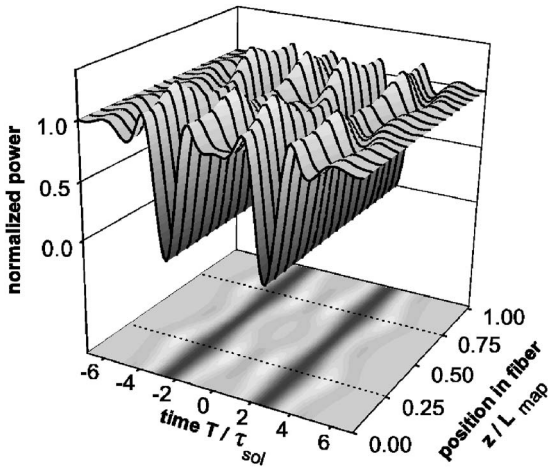

FIG. 2. Propagation of a pair of dark solitons at separation $\Delta T/\tau_{\mathrm{sol}}=5.0$ over one dispersion map period. The dispersion is $\beta_2=\beta_+$ for $0\leqslant z<0.25$ and $0.75<z\leqslant 1$, and $\beta_2=\beta_-$ for $0.25<z<0.75$. The undulations in the wings move somewhat, but the position of the centers is very nearly constant.

zeroes is plotted as a function of their position in the transmission line. Each line describes the evolution of the separation between dark DM solitons along the fiber for one particular initial separation, ranging from 0.9 τ_{sol} to 9.8 τ_{sol}. Remarkably, starting from this quasicontinuum of initial separations the curves tend to a set of five fixed final separations which are highlighted by arrows in Fig. 1. These fixed normalized separations $\Delta T/\tau_{\mathrm{sol}}$ constitute a set of "magic numbers" which we will refer to below repeatedly. Bound pairs of dark solitons exist at separations corresponding to one of the magic numbers.

On closer inspection one notes that individual traces approach these equilibrium positions in an oscillatory fashion: this implies that there is not only repulsion but also attraction, and some kind of binding energy so that certain separations are stabilized. The oscillation period, being a rough indicator of the strength of the binding force, becomes longer for growing initial separation. This shows that the binding force falls with distance; at separations more than 10 τ_{sol} it has practically vanished.

The bound dark soliton pair undergoes some breathing over a dispersion map period L_{map}. The separation of the centers is modulated only slightly in the case of the narrowest separation $\Delta T/\tau_{\mathrm{sol}}=1.3$, and almost unnoticeably for the larger separations. Figure 2 presents the case of the third magic number 5.0. In the following we will show propagations in a stroboscopic manner, i.e., only at the half-segment points. There the width of the minima in the bound state is slightly different from τ_{sol}: it is 9% narrower for the smallest magic number, 5% wider for the second, and for the others $\leqslant 1\%$ wider.

We turn to an interpretation of the origin of the repulsive and attractive behavior by taking a closer look at the pulse shape of the dark DM solitons. As pointed out in Ref. [25], the wings of dark DM solitons carry undulations; the undulation amplitude increases with growing map strength. Figure 3 shows the shape of a dark DM soliton pair and its decomposition into two individual dark DM solitons with their undulations. We observe that stable separations correlate with certain relative positions of the undulations: The relative positions move somewhat across one dispersion map period, but at the position where they are shown (the "chirp-free" point at the center of L_+) the undulations of the two

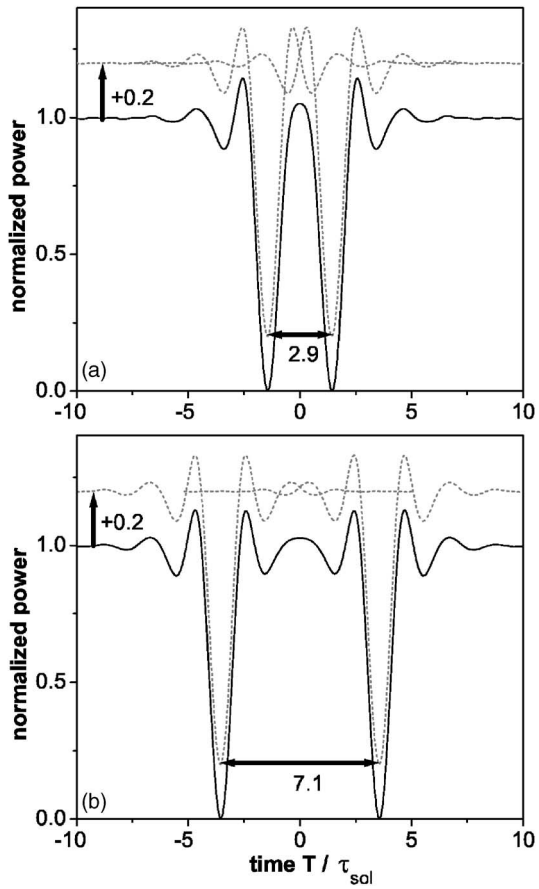

FIG. 3. Dark soliton pairs and their constituents. Separation $\Delta T/\tau_{\mathrm{sol}}$ equals (a) 2.9, (b) 7.1. Solid black line: dark soliton pair. Dashed gray line: two single position-shifted dark DM solitons.

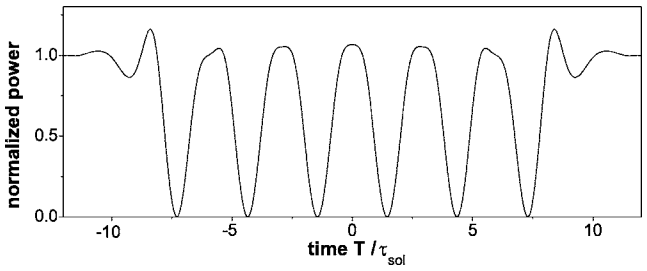

FIG. 4. Chain of six dark DM solitons. A suitable initial condition was propagated over 63 dispersion lengths to yield the trace shown.

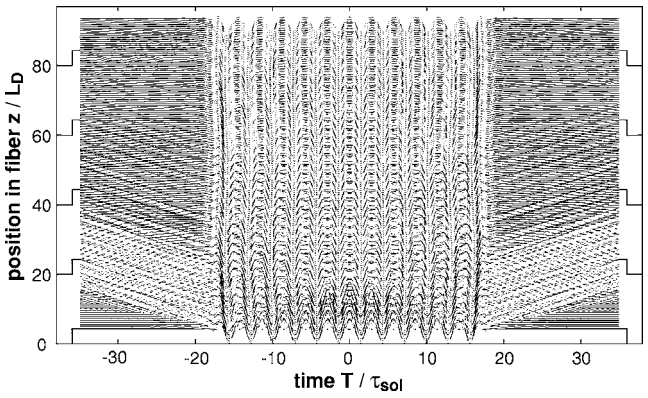

FIG. 5. Stable propagation of a chain of 12 dark solitons. The separation was chosen as 2.9 (compare Fig. 1). Propagation (from bottom to top trace) is shown over 300 dispersion map periods or $93L_D$ as defined in the text. Measurement in high-resolution enlargements reveal that radiation moves out at a speed of $1.43\tau_{sol}/L_D$ outside, $1.11\tau_{sol}/L_D$ inside the chain.

dark solitons overlap almost in antiphase; throughout one dispersion map they remain near this condition. The same is found for all magic numbers. While details of the mechanism remain to be understood, it is obvious that the undulations in the wings of the dark DM solitons are responsible for the interaction forces between the solitons.

VI. DARK SOLITON CHAINS

To generate multiple dark solitons we use the product of several position-shifted hyperbolic-tangent pulses as described above as a launching condition—again, a rough approximation to the structure that finally emerges. This structure has a power profile like a comb of dark pulses. For Fig. 4 we chose six dark pulses and the second magic number 2.9 as their mutual separation, and had it propagate over 63 dispersion lengths, certainly a more than sufficient distance for transients to die out. It turns out that the dark pulses maintain their position with respect to each other. In other words, the dark soliton comb propagates quasistably. To emphasize that the solitons in the comb lock in at certain separations, we speak of *chains*. We have obtained chains consisting of up to twelve dark DM solitons so far, and emphasize that a limitation of the chain length is not apparent yet: we were limited so far by the available computational power.

In Fig. 5 we show the propagation of a 12-soliton chain over a very long distance. Here the second magic number 2.9 was chosen for the mutual separation. Apparently this chain is remarkably stable. We also find quasistable propagation over the distance considered for the other magic numbers with the exception of the smallest 1.3. In that case the chain breaks apart after only part of the propagation distance shown. Our interpretation is that at this closest separation of a pair, the separation is not quite constant in the course of one dispersion period but oscillates around it by a few percent. As the chain gets longer, one soliton pushes the next in the row, and the outermost solitons must undergo a correspondingly larger oscillation around their average position. Eventually the perturbation becomes so large that it compromises stability. Quite generally we find that positional perturbations of more than several percent of the separation are too strong, so that the chain may break into fragments: either shorter chains or individual dark pulses.

Since our launch condition is only approximating the shape of the chain, some radiation must be shed in the transition phase. This is easily visible in Fig. 5 as small waves radiating out on either side with fixed speed. It is also plainly visible that initially much more is radiated than later on. An interesting observation is that the speed at which the radiation moves out is different inside and outside the chain. High-resolution enlargements of Fig. 5 allow direct reading of the angle at which maxima move out (i.e., the speed), both outside and also inside the dark soliton chain. We find that the speed is $1.11\tau_{sol}/L_D$ inside, as compared to $1.43\tau_{sol}/L_D$ outside. (Note that the speed here has unusual dimension and units: radiation moves out on the time axis as the structure propagates down the fiber; hence, speed has dimensions of time per length.) If one is willing to interpret the soliton chain as a kind of one-dimensional soliton crystal [35], this indicates that the crystal has a refractive index different from that of the outside. This interpretation is in accord with our observation that the speed depends on the separation. At larger separation (lower density) the speed inside is closer to the speed outside. For example, for a separation of 5.0 we find a value of $1.33\tau_{sol}/L_D$. In other words: in the dense crystal the speed is 78%, in the less dense crystal 93% of the outside value.

There is no requirement that all nearest-neighbor distances in the chain are equal. We can freely select separations from the list of magic numbers given in Fig. 1. Fig. 6 shows an example of a chain of eight dark solitons in which three have a separation of 2.9, the other of 5.0. This compound propagates quasistably, too. Again, the different speed of relative motion of dispersive waves take the different values described above in the two zones and on the outside. We have convinced ourselves that also randomly chosen selections of different magic number nearest-neighbor separations yield quasistable chains.

VII. DISCUSSION AND CONCLUSION

We have demonstrated an attractive interaction between dark DM solitons. This attraction is mediated by undulations

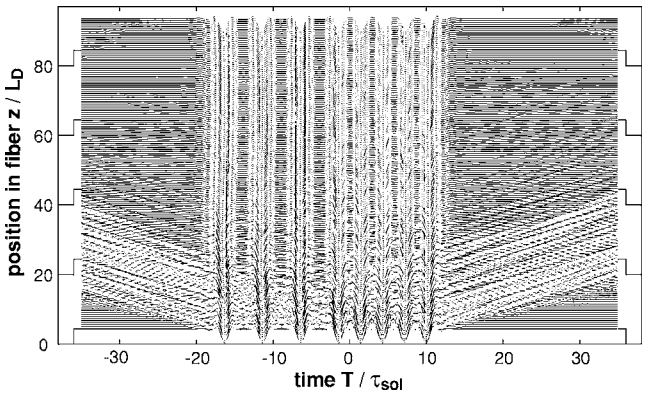

FIG. 6. Chain of dark solitons with unequal separations: In contrast to Fig. 5 the separation is 5.0 in the left half, 2.9 in the right half. Radiation moves out at a speed of $1.43\tau_{\mathrm{sol}}/L_{\mathrm{D}}$ outside as before, $1.11\tau_{\mathrm{sol}}/L_{\mathrm{D}}$ inside the denser portion and $1.33\tau_{\mathrm{sol}}/L_{\mathrm{D}}$ inside the less dense portion of the chain.

in their wings. In combination with the previously known repulsive interaction an equilibrium of forces can be established which gives rise to bound states of dark solitons. Several quasistable separations are possible, but the degree of stability is reduced with increasing separation. The bound states are in no way restricted to pairs of solitons: chains of up to twelve stably bound dark solitons have been shown, and even longer chains may be possible.

Attraction between dark solitons was considered impossible in fiber optics, but in different contexts it has been described before. In Ref. [36] the repulsive interaction of spatial vector solitons was compensated by bright light in between; this compensating action was likened to gluonic interaction. In Ref. [37] it was shown that nonlocal interaction can lift the repulsive interaction. We demonstrate attraction between same-frequency, same-polarization fiber-optic dark solitons in dispersion-managed fiber.

In the simplest case, i.e. when the nearest-neighbor distance is the same everywhere throughout the chain, all possible chains form a two-parameter family: the number of participating solitons can vary from one to at least 12, and possibly many more, and the nearest-neighbor distance can take one out of five (or possibly more) discrete values (the magic numbers). It stands to reason that in the limiting case of infinitely many participating solitons and for one particular distance, one approaches the limiting case of the snoidal wave described in [30]. Further research will make this conjecture more specific. Our result is much more general, though, because it presents the entire transition from single-soliton to multisoliton objects with different separations. Beyond that, one can even have chains with nonuniform spacings. The resulting enormous number of different chain arrangements, reminiscent of bar codes, may constitute yet another way to encode information.

ACKNOWLEDGMENTS

This work was financially supported in the framework of DIP 6.6 (Deutsch-Israelische Projektpartnerschaft). We benefited from interactions with Michael Böhm and Haldor Hartwig.

[1] A. Hasegawa and F. Tappert, Appl. Phys. Lett. **23**, 142 (1973).
[2] L. F. Mollenauer, R. H. Stolen, and J. P. Gordon, Phys. Rev. Lett. **45**, 1095 (1980).
[3] V. E. Zakharov and A. B. Shabat, Sov. Phys. JETP **34**, 62 (1971).
[4] G. P. Agrawal, *Nonlinear Fiber Optics* (Academic Press, San Diego, 1995).
[5] C. R. Menyuk, J. Opt. Soc. Am. B **10**, 1585 (1993).
[6] P. Emplit, J. P. Hamaide, F. Reynaud, C. Froehly, and A. Barthelemy, Opt. Commun. **62**, 374 (1987).
[7] D. Krökel, N. J. Halas, G. Giuliani, and D. Grischkowsky, Phys. Rev. Lett. **60**, 29 (1988).
[8] A. M. Weiner, J. P. Heritage, R. J. Hawkins, R. N. Thurston, E. M. Kirschner, D. E. Leaird, and W. J. Tomlinson, Phys. Rev. Lett. **61**, 2445 (1988).
[9] M. Haelterman and P. Emplit, Electron. Lett. **29**, 356 (1993).
[10] W. Zhao and E. Bourkoff, Opt. Lett. **14**, 703 (1989).
[11] M. Lisak, D. Anderson, and B. A. Malomed, Opt. Lett. **16**, 1936 (1991).
[12] J. P. Hamaide, P. Emplit, and M. Haelterman, Opt. Lett. **16**, 1578 (1991).
[13] Y. S. Kivshar, M. Haelterman, P. Emplit, and J. P. Hamaide, Opt. Lett. **19**, 19 (1994).
[14] W. Zhao and E. Bourkoff, Opt. Lett. **14**, 1371 (1989).
[15] F. Mitschke and L. F. Mollenauer, Opt. Lett. **11**, 659 (1986).
[16] Y. S. Kivshar and V. V. Afanasjev, Opt. Lett. **16**, 285 (1991).
[17] I. M. Uzunov and V. S. Gerdjikov, Phys. Rev. A **47**, 1582 (1993).
[18] V. Aleshkevich, Y. Kartashov, and V. Vysloukh, J. Opt. Soc. Am. B **18**, 1127 (2001).
[19] H. J. Shin, J. Phys. A **38**, 3307 (2005).
[20] J. H. B. Nijhof, N. J. Doran, W. Forysiak, and F. M. Knox, Electron. Lett. **33**, 1726 (1997).
[21] Y. Chen and H. A. Haus, Opt. Lett. **23**, 1013 (1998).
[22] S. K. Turytsin and E. G. Shapiro, Opt. Lett. **23**, 682 (1998).
[23] J. N. Kutz and S. G. Evangelides, Opt. Lett. **23**, 685 (1998).
[24] V. S. Grigoryan and C. R. Menyuk, Opt. Lett. **23**, 609 (1998).
[25] M. Stratmann, M. Böhm, and F. Mitschke, Electron. Lett. **37**, 1182–1183 (2001).
[26] M. J. Ablowitz and Z. H. Musslimani, Phys. Rev. E **67**, 025601(R) (2003).
[27] M. Böhm and F. Mitschke, Appl. Phys. B **81**, 983 (2005).
[28] M. Stratmann, T. Pagel, and F. Mitschke, Phys. Rev. Lett. **95**, 143902 (2005).
[29] Y. V. Kartashov, V. A. Aleshkevich, V. A. Vysloukh, A. A. Egorov, and A. S. Zelenina, Phys. Rev. E **67**, 036613 (2003).
[30] Y. V. Kartashov, V. A. Vysloukh, E. Marti-Panameño, D. Artigas, and L. Torner, Phys. Rev. E **68**, 026613 (2003).
[31] K. J. Blow and N. J. Doran, Phys. Lett. **107A**, 55 (1985).
[32] D. Foursa and P. Emplit, Phys. Rev. Lett. **77**, 4011 (1996).

[33] C. Paré and P.-A. Bélanger, Opt. Commun. **168**, 103–109 (1999).
[34] A. Maruta, T. Inoue, Y. Nonaka, and Y. Yoshika, IEEE J. Sel. Top. Quantum Electron. **8**, 640 (2002).
[35] F. Mitschke and A. Schwache, Quantum Semiclassic. Opt. **10**, 779 (1998).
[36] E. A. Ostrovskaya, Y. S. Kivshar, Z. Chen, and M. Segev, Opt. Lett. **24**, 327 (1999).
[37] N. I. Nikolov, D. Neshev, W. Krolikowski, O. Bang, J. J. Rasmussen, and P. L. Christiansen, Opt. Lett. **29**, 286 (2004).